Metamorphism of the Lower Palaeozoic rocks of the Builth Wells district, Wales, 1:50k sheet 196

Integrated Geoscience Surveys Southern Programme

Internal Report IR/02/025

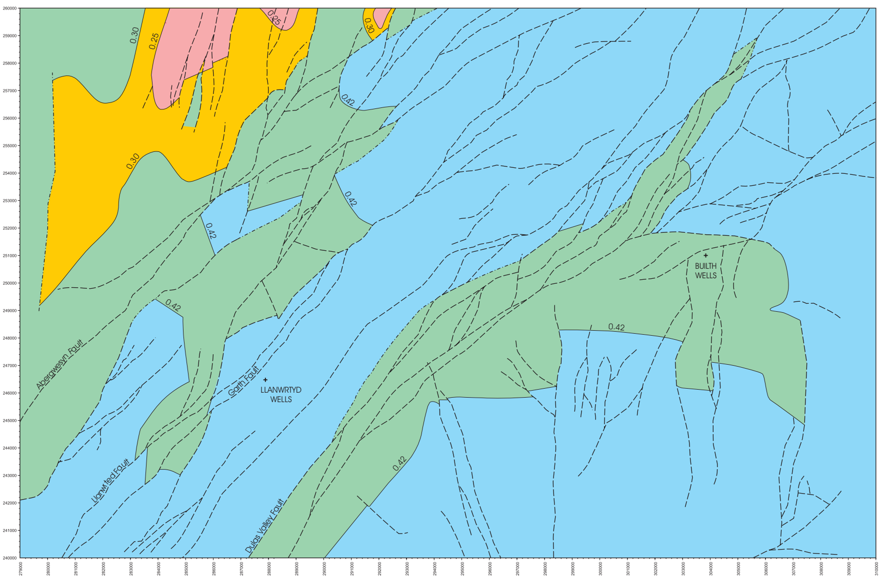

BRITISH GEOLOGICAL SURVEY

INTERNAL REPORT IR/02/025

Metamorphism of the Lower Palaeozoic rocks of the Builth Wells district, Wales, 1:50k sheet 196

S J Kemp and R J Merriman

Key words

Low grade metamorphism, mica (illite) crystallinity.

Front cover

Contoured metamorphic map of white mica crystallinity (Kubler) indices for the Builth Wells district.

Bibliographical reference

KEMP, S J AND MERRIMAN, R J. 2002. Metamorphism of the Lower Palaeozoic rocks of the Builth Wells district, Wales, 1:50k sheet 196. *British Geological Survey Internal Report*, IR/02/025. 18pp.

Keyworth, Nottingham British Geological Survey 2002

BRITISH GEOLOGICAL SURVEY

The full range of Survey publications is available from the BGS Sales Desks at Nottingham and Edinburgh; see contact details below or shop online at www.thebgs.co.uk

The London Information Office maintains a reference collection of BGS publications including maps for consultation.

The Survey publishes an annual catalogue of its maps and other publications; this catalogue is available from any of the BGS Sales Desks.

The British Geological Survey carries out the geological survey of Great Britain and Northern Ireland (the latter as an agency service for the government of Northern Ireland), and of the surrounding continental shelf, as well as its basic research projects. It also undertakes programmes of British technical aid in geology in developing countries as arranged by the Department for International Development and other agencies.

The British Geological Survey is a component body of the Natural Environment Research Council.

Keyworth, Nottingham NG12 5GG

☎ 0115-936 3241 Fax 0115-936 3488
e-mail: sales@bgs.ac.uk
www.bgs.ac.uk
Shop online at: www.thebgs.co.uk

Murchison House, West Mains Road, Edinburgh EH9 3LA

☎ 0131-667 1000 Fax 0131-668 2683
e-mail: scotsales@bgs.ac.uk

London Information Office at the Natural History Museum (Earth Galleries), Exhibition Road, South Kensington, London SW7 2DE

☎ 020-7589 4090 Fax 020-7584 8270
☎ 020-7942 5344/45 email: bgslondon@bgs.ac.uk

Forde House, Park Five Business Centre, Harrier Way, Sowton, Exeter, Devon EX2 7HU

☎ 01392-445271 Fax 01392-445371

Geological Survey of Northern Ireland, 20 College Gardens, Belfast BT9 6BS

☎ 028-9066 6595 Fax 028-9066 2835

Maclean Building, Crowmarsh Gifford, Wallingford, Oxfordshire OX10 8BB

☎ 01491-838800 Fax 01491-692345

Parent Body
Natural Environment Research Council, Polaris House, North Star Avenue, Swindon, Wiltshire SN2 1EU

☎ 01793-411500 Fax 01793-411501
www.nerc.ac.uk

Foreword

This report is the published product of a study by the British Geological Survey (BGS) and forms part of the Core Strategic (Lands and Resources) Programme.

Acknowledgements

We are grateful to David Schofield, Dick Waters and David Wilson for providing a draft geological map and advice on the interpretation of the metamorphic data.

Contents

FIGURES

Summary

The pattern of regional metamorphism indicated by illite crystallinity has been used to interpret the tectonic and thermal history of the Builth Wells district. Grade generally increases from the southeast of the district towards the northwest. The Abergwesyn Fault separates an area of mainly late diagenetic rocks in the southeast of the district from high-anchizone and epizonal rocks in the northwest. The lowest grade rocks southeast of the Abergwesyn Fault are largely the result of burial metamorphism under a pre-tectonic overburden 4-5.5 km thick. A slate belt in the northwest of the district was generated by deformation associated with the Acadian Orogeny. Peak metamorphic temperatures of 300°C developed under a tectonic overburden 6-8 km thick.

1 Introduction

As part of the geological survey of the Builth Wells district, mudrock lithologies (mudstone and slate) representing the main stratigraphical units were sampled and analysed to determine *illite crystallinity (IC)* indices. Illite crystallinity provides an indication of *metapelitic grade*, and the distribution of grades can be used to interpret the tectonic and geothermal history of low-grade metamorphic terrains. This report gives details of the methods used and presents the results as a contoured metamorphic map that is used to interpret the metamorphic history of the district.

2 Techniques and laboratory methods

2.1 TECHNIQUES

Clay minerals are characterised by very small crystals with the ability to attract or release water and other chemical elements in their crystal structure. Such properties enable clays to react relatively rapidly to changes in temperature and pressure in the upper part of the Earth's crust. Clay mineral reactions begin with the burial and progressive compaction of unconsolidated clays in basinal sequences, and these diagenetic processes produce a lithified mudstone. The clay mineral reactions that accompany lithification transform authigenic minerals, such as smectite and kaolinite, to assemblages dominated by illite and chlorite. Tectonic deformation of mudstone results in further progressive changes in clay mineral assemblages and the development of a *slaty cleavage microfabric*. Slates with a pervasive slaty cleavage microfabric contain white mica crystallite populations that are 2-3 times thicker than those found in typical mudstones. The increase in crystallite thickness associated with slaty cleavage microfabric is a response to several interactive processes, including mechanical grain rotation, pressure-solution crystallization and grain-boundary migration (dislocation creep), collectively referred to as *strain-related crystal growth* (Merriman & Peacor, 1999).

Progress of late diagenetic and very low grade metamorphic reactions in buried and tectonized mudrock sequences can be monitored by measuring changes in the illite–muscovite (white mica) reaction series as thicker crystallites develop in response to progressive recrystallisation (Merriman *et al.*, 1990; Warr & Nieto, 1998). The *Kubler index (KI in $\Delta°2\theta$)* measures small reductions in the half-height width of the mica ~10 Å XRD (X-ray diffraction) peak which occur when the crystallite population thickens. In mudrock sequences the Kubler index is used to define the limits of a series of metapelitic zones of very low– and low-grade metamorphism: late diagenetic zone KI>0.42; low-anchizone KI 0.30–0.42; high-anchizone KI 0.25–0.30; epizone KI<0.25 (Merriman & Peacor, 1999).

For this study, 158 mudrocks were collected from the area within Sheet 196. The results from samples collected along the margins of the surrounding sheets were also included to ensure the connectivity of isocrysts. This represents a sampling density of approximately one mudrock per 4 km^2. All samples were prepared and analysed by XRD techniques in order to determine the Kubler index (KI) of illite crystallinity.

2.2 SAMPLE PREPARATION

After removing any surface contaminants with a wire brush, a representative 50 g portion of each sample was stage-ground, using a Cr-steel tema-mill in 5 second bursts, to pass a 1 mm sieve. Care was taken to subject the sample to short bursts of milling in order to reduce the chance of over-grinding delicate *phyllosilicate* grains.

A representative 4 g portion of each <1 mm crushed sample was then placed in a boiling tube and distilled water added to a predetermined level. Each sample was then shaken thoroughly, subjected to ultrasound for 5 minutes and allowed to stand for 3 hours. Where flocculation occurred, 0.5 ml of 0.1M sodium hexametaphosphate was added and the dispersion process repeated. After 3 hours, a nominal <2 μm fraction was removed and centrifuged at maximum speed for 20 minutes. The clear supernatant was then removed and the <2 μm fraction re-dispersed in ~1 ml distilled water with a glass rod and minimal ultrasound. The <2 μm fraction slurry was then pipetted onto the surface of a frosted glass slip and allowed to dry overnight at room temperature.

2.3 X-RAY DIFFRACTION ANALYSIS

Each glass slip was analysed using a Philips PW1130 series diffractometer equipped with Ni-filtered Cu-Kα radiation and operating at 40kV and 30mA. The KIs of the samples were calculated from the mean of five scans over the range 7.5-10.5 °2θ at a speed of 0.5 °2θ/minute using the machine conditions recommended by Kisch (1991). The width of the ~10 Å peak at half-height was measured using Hiltonbrooks software modified by N J Fortey (BGS) and values were adjusted to concur with previous measurements carried out at Birkbeck College, University of London, using the crystallinity index standards (CIS) of Warr & Rice (1994).

3 Metamorphic map

The metamorphic map shown in Figure 2 is the result of computer contouring of KI data, which was subsequently manually modified to reflect the influence of localized post–metamorphic faulting. A computer contoured geographical distribution of KI datapoints was initially produced using DeltaGraph Professional 4.0 for Windows software. The pattern was then superimposed on an outline 1:50k geological map of the Lower Palaeozoic rocks and contours redrawn where late faulting appeared to modify the overall pattern. In the final version of the map shown in Figure 1, contours of equal crystallinity (isocrysts), or faults where they coincide, are used to delineate four metapelitic zones: late diagenetic zone (KI >0.42); low-anchizone (KI 0.30–0.42); high-anchizone (KI 0.25–0.30) and epizone (<0.25). The errors and precision involved in contouring the crystallinity data (Robinson *et al.*, 1990), have been previously determined by multi–sampling at several sites in Wales and elsewhere (Roberts *et al.*, 1990; Merriman & Roberts, 1992). The results from multi–sampled sites indicate that 95% of the samples have indices within the range of values delineated by zonal isocrysts.

The overall pattern of regional metamorphism shows a general increase in grade from the basin margin in the southeast of the district to the more deeply subsided basin centre in the northwest. As a result, some of the oldest Ordovician rocks forming the Builth Inlier are at lower grades than younger Silurian strata on the SE limb of the Central Wales Syncline.

The district is divided into low-grade and very low-grade areas on either side of the Abergwesyn Fault. Very low-grade mudrocks on the southeast side of the Abergwesyn Fault are predominantly in the late diagenetic zone, where burial temperatures were probably less than 200°C. The late diagenetic zone rocks include those of Ordovician age, forming the Tywi Lineament, and the Devonian strata cropping out in the southeast of the district. Slaty cleavage microfabric is absent or very weakly developed in these late diagenetic zone pelites. Rocks belonging to the low-anchizone are found between the Abergwesyn and Garth faults, and in the fault zone of the Pontesford Lineament. The higher grades indicated by the low-anchizone are likely to reflect the initial stage of development of slaty cleavage microfabric. This poorly developed cleavage may be a response to shearing and relatively high strain-rates within the Pontesford Lineament fault zone. Northwest of the Abergwesyn Fault, grade is mostly in the high-anchizone or epizone. Highest grade epizonal rocks occur in the more intensely folded strata forming the southwesterly closure of the Rhiwnant Anticline and, on its SE-limb, the Gwesyn Syncline. Within this fold-pair, grade has been increased by strain-related crystal growth associated with the development of a penetrative slaty cleavage.

4 Metamorphic history

Published studies of various aspects of the metamorphic history of the Welsh Basin suggest that there were two main regional episodes: an early burial metamorphism related to the extensional phase of basin evolution, followed by tectonothermal metamorphism related to the contraction and uplift of the basin (Merriman & Frey, 1999).

The evidence for burial metamorphism has been inferred from the approximate parallelism of formation boundaries and contoured illite crystallinity data in the rocks to the north of the Builth district (Roberts *et al.*, 1996). In addition, transmission electron microscope (TEM) studies show that thin crystals of white mica and chlorite generated by burial metamorphism develop a bedding-parallel orientation (Li *et al.*, 1994). Within the Builth district, the absence of a well-developed slaty cleavage indicates that much of the area to the southeast of the Abergwesyn Fault is the result of burial metamorphism. Estimates of the palaeogeothermal gradient during burial metamorphism to the north of the district are in the range 36-52°C km^{-1} (Roberts *et al.*, 1996). These suggest that pre-tectonic overburden thicknesses were in the range 4-5.5 km in this part of the Welsh Basin.

A pattern of metamorphism closely related to deformation was superimposed on the burial pattern when the Welsh Basin contracted and inverted during the Acadian Orogeny. Where deformation was most intense, a combination of strain and thermal energy promoted crystal thickening of white mica in a pervasive slaty cleavage fabric. The slate belts generated by this metamorphic episode are typically in the epizone or high anchizone, such as those associated with the Tylwch anticline, the common limb of the Teifi anticline and Central Wales syncline, to the north and northwest of the Builth district (Davies *et al.*, 1997). An extension of the slate belt associated with the Rhiwnant Anticline and Gwesyn Syncline occupies the northwestern part of the district. Here metamorphic temperatures are inferred to have reached 300°C under an overburden thickened by folding. Using the palaeogeothermal gradients discussed above, the inferred thickness of the tectonic overburden was in the range 6-8 km.

5 References

Most of the references listed below are held in the Library of the British Geological Survey at Keyworth, Nottingham. Copies of the references may be purchased from the Library subject to the current copyright legislation.

DAVIS, J R, FLETCHER, C J N, WATERS, R A, WILSON, D, WOODHALL, D G, and ZALASIEWICZ, J A. 1997. Geology of the country around Llanilar and Rhayader. *Memoir of the British Geological Survey*, Sheets 178 &179 (England & Wales). HMSO, London.

KISCH, H J. 1991. Illite crystallinity: recommendations on sample preparation, X-ray diffraction settings and interlaboratory standards. *Journal of Metamorphic Geology*, **9**, 665-670.

LI, G, PEACOR, D R, MERRIMAN, R J and ROBERTS, B. 1994. The diagenetic to low grade metamorphic evolution of matrix white micas in the system muscovite-paragonite in a mudrock from Central Wales, U.K. *Clays and Clay Minerals*, **42**, 369-381.

MERRIMAN, R J, and ROBERTS, B. 1992. The low grade metamorphism of Lower Palaeozoic strata on the Rhins of Galloway, SW Scotland. *British Geological Survey Technical Report* **WG/92/40**.

MERRIMAN, R J, and FREY, M. 1999. Patterns of very low–grade metamorphism in metapelitic rocks. 61-107 in *Low–grade Metamorphism.* FREY, M and ROBINSON, D. (editors). Blackwell Science.

MERRIMAN, R J, and PEACOR, D R. 1999. Very low–grade metapelites: mineralogy, microfabrics and measuring reaction progress. 10-60 in *Low–grade Metamorphism.* FREY, M and ROBINSON, D. (editors). Blackwell Science.

MERRIMAN, R J, ROBERTS, B, and PEACOR, D R. 1990. A transmission electron microscope study of white mica crystallite size distribution in a mudstone to slate transitional sequence, North Wales, U K. *Contributions to Mineralogy and Petrology*, **10,** 27-40.

ROBERTS, B, MORRISON, C, and HIRONS, S. 1990. Low grade metamorphism of the Manx Group, Isle of Man: a comparative study of white mica 'crystallinity' techniques. *Journal of the Geological Society of London*, **147**, 271-277.

ROBERTS, B, MERRIMAN, R J, HIRONS, S R, FLETCHER, C J N, and WILSON, D. 1996. Synchronous very low grade metamorphism, contraction and inversion in the central part of the Welsh Lower Palaeozoic Basin. *Journal of the Geological Society, London*, **153**, 277-286.

ROBINSON, D, WARR, L, and BEVINS, R E. 1990. The illite 'crystallinity' technique: a critical appraisal of its precision. *Journal of Metamorphic Geology*, **8**, 333-344.

WARR, L, and RICE, A H N. 1994. Interlaboratory standardization and calibration of clay mineral crystallinity and crystallite size data. *Journal of Metamorphic Geology*, **12**, 141–152.

WARR, L, and NIETO, F. 1998. Crystallite thickness and defect density of phyllosilicates in low-temperature metamorphic pelites: a TEM and XRD study of clay-mineral crystallinity-index standards. *The Canadian Mineralogist*, **36**, 1453-1474.

Glossary

Illite crystallinity (IC) Variations in the crystallite size and lattice strain in dioctahedral mica produced in the smectite-I/S-illite-muscovite reaction series, as indicated by the Kubler index.

Kubler index (KI) The width of the X-ray diffraction c.10Å peak at half-height above background, measured as small changes in the Bragg angle $\Delta°2\theta$.

Metapelitic grade The grade of diagenesis and low-grade metamorphism indicated by reaction progress in clay minerals and other phyllosilicates.

Slaty cleavage microfabric A pervasive planar fabric consisting of submicron-spaced domains of phyllosilicates. Strain-related crystal growth of the phyllosilicates has resulted in their (00l) crystallographic planes being orientated approximately parallel to the fabric. Although the mineral constituents of the microfabric cannot be resolved with the naked eye, their parallel orientation gives rise to a fissility that dominates all other fabric elements of the mudrock and can be exploited to cleave the rock into thin (<10 mm) parallel-sided slates.

Strain-related crystal growth The crystal growth of minerals induced by rock deformation. Strain-related crystal growth is response to several interactive processes, including mechanical grain rotation of existing minerals, pressure-solution (dissolution) recrystallization and grain-boundary migration (dislocation creep) in newly-formed minerals.

Phyllosilicates A group of silicate minerals, including the micas and clay minerals, which consist of SiO_4 tetrahedra linked into flat sheets with an Si:O ratio of 1:5. Cations and water are accommodated between the sheets and such minerals are characterised by a very prominent cleavage parallel to the sheet structure.

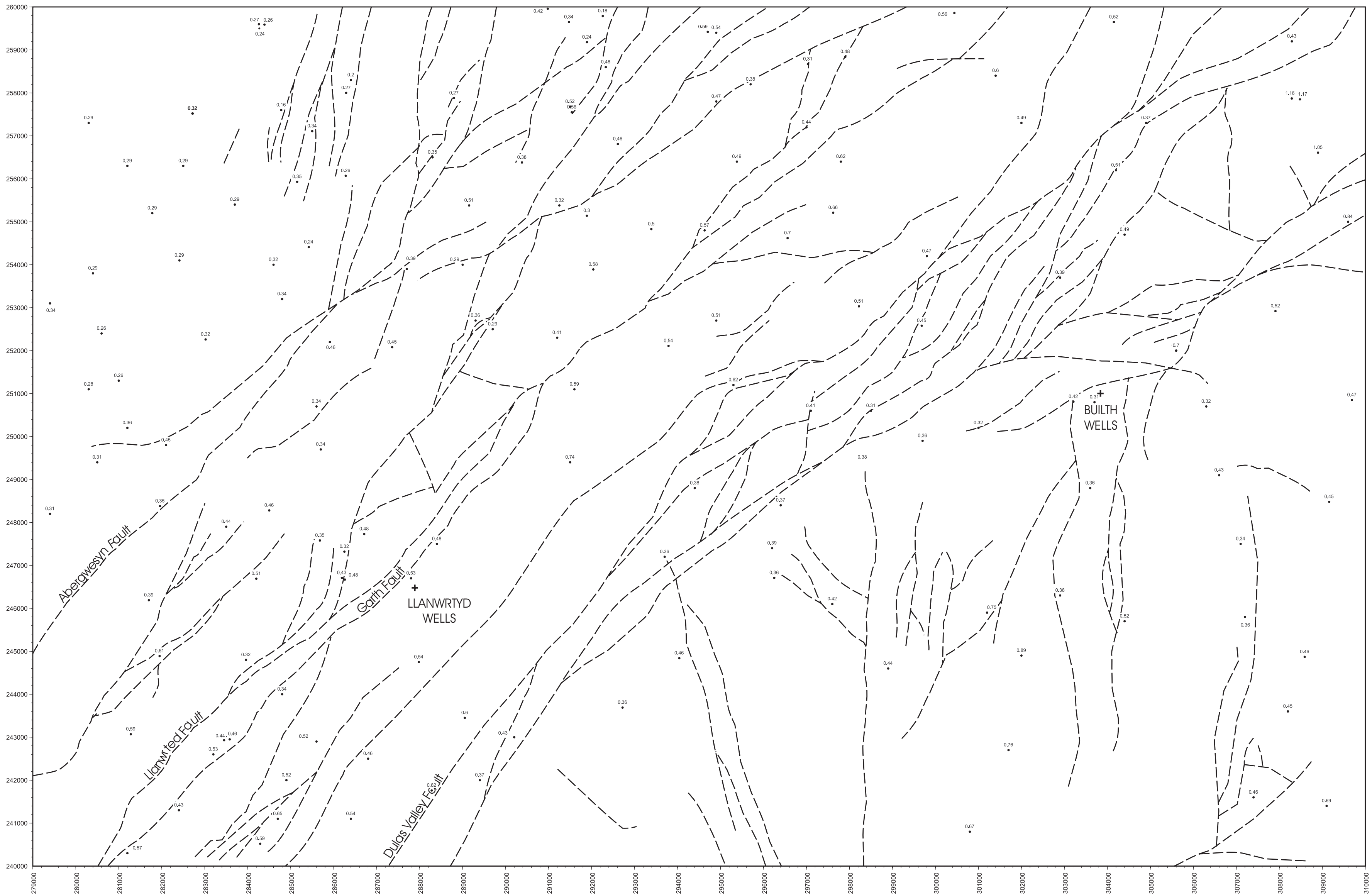

Figure 1. Sample location map and white mica crystallinity (Kubler) indices for the Builth Wells district

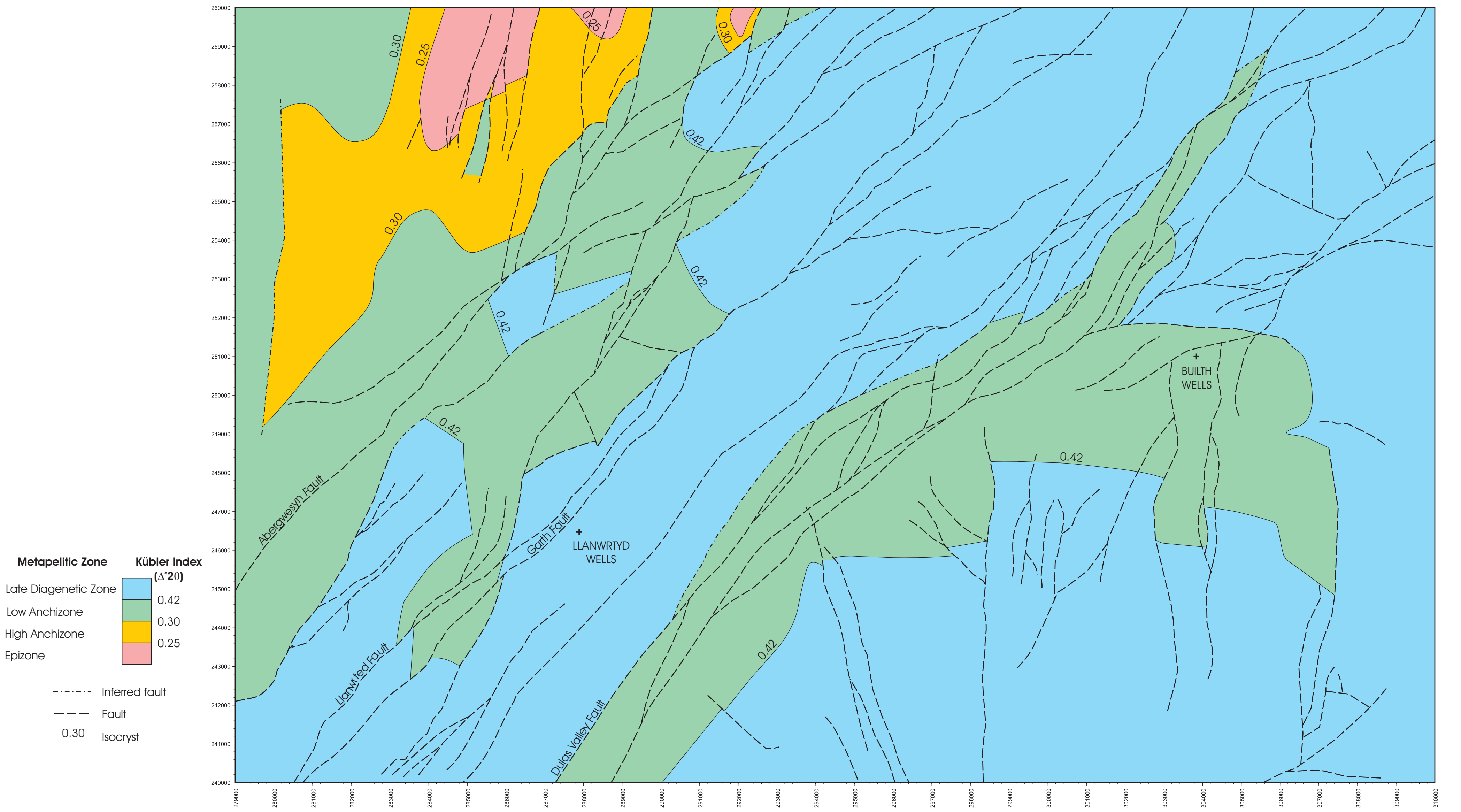

Figure 2. Contoured metamorphic map of white mica crystallinity (Kubler) indices for the Builth Wells district.

Appendix 1 Summary of sample numbers, sample locations and KIs

Sample No.	Square	Easting	Northing	IC	Sample No.	Square	Easting	Northing	IC
BRM0777	SN	287800	259900	0.25	BRM1735	SO	301700	242700	0.76
BRM0791	SN	284390	259590	0.26	BRM1736	SO	302000	244900	0.89
BRM0792	SN	284270	259500	0.24	BRM1737	SO	303600	248800	0.36
BRM0793	SN	284260	259600	0.27	BRM1738	SO	301200	245900	0.75
BRM1157	SO	308300	259200	0.43	BRM1739	SO	302900	246300	0.38
BRM1166	SO	300440	259860	0.56	BRM1740	SO	304400	245700	0.52
BRM1167	SN	282870	258830	0.30	BRM1741	SO	308200	243600	0.45
BRM1244	SN	292260	259790	0.18	BRM1742	SO	307200	245800	0.36
BRM1245	SN	290980	259960	0.42	BRM1743	SO	307100	247500	0.34
BRM1249	SN	291480	259650	0.34	BRM1744	SO	306600	249100	0.43
BRM1250	SN	291900	259180	0.24	BRM1745	SO	306300	250700	0.32
BRM1251	SN	294710	259420	0.59	BRM1746	SO	305600	252000	0.65
BRM1252	SN	298590	257490	0.55	BRM1747	SO	305600	252000	0.70
BRM1253	SN	297040	258670	0.31	BRM1749	SO	309600	255000	0.84
BRM1255	SN	297910	258840	0.48	BRM1751	SO	304900	257300	0.37
BRM1694	SN	298500	250600	0.31	BRM1752	SO	304200	256200	0.51
BRM1695	SN	291200	252300	0.41	BRM1753	SO	304400	254700	0.49
BRM1696	SN	289700	252500	0.29	BRM1755	SO	302900	253700	0.39
BRM1697	SN	289300	252700	0.36	BRM1756	SO	302000	257300	0.49
BRM1698	SN	289000	254000	0.29	BRM1757	SO	301400	258400	0.60
BRM1699	SN	287700	253900	0.39	BRM1758	SN	297800	256400	0.62
BRM1700	SN	284800	253200	0.34	BRM1759	SN	297000	257200	0.44
BRM1701	SN	284600	254000	0.32	BRM1760	SN	295700	258200	0.38
BRM1702	SN	283700	255400	0.29	BRM1761	SN	299800	254200	0.47
BRM1703	SN	282500	256300	0.29	BRM1762	SN	293700	247200	0.36
BRM1704	SN	281200	256300	0.29	BRM1763	SN	286400	241100	0.54
BRM1705	SN	280300	257300	0.29	BRM1764	SN	284700	241100	0.65
BRM1707	SN	291600	251100	0.59	BRM1765	SN	284900	242000	0.52
BRM1708	SN	288400	247500	0.48	BRM1766	SN	285600	242900	0.52
BRM1709	SN	285700	249700	0.34	BRM1767	SN	286800	242500	0.46
BRM1710	SN	285600	250700	0.34	BRM1768	SN	289400	242000	0.37
BRM1711	SN	280300	251100	0.28	BRM1769	SN	290200	243000	0.43
BRM1712	SN	280400	253800	0.29	BRM1770	SN	291500	249400	0.74
BRM1713	SN	279400	253100	0.34	BRM1771	SN	294400	248800	0.38
BRM1714	SN	280600	252400	0.26	BRM1772	SN	297100	250600	0.41
BRM1715	SN	281000	251300	0.26	BRM1773	SN	295300	251200	0.62
BRM1716	SN	281200	250200	0.36	BRM1774	SN	294900	252700	0.51
BRM1717	SN	282100	249800	0.45	BRM1775	SN	294900	257800	0.47
BRM1718	SN	280500	249400	0.31	BRM1776	SN	294900	259400	0.54
BRM1719	SN	279400	248200	0.31	BRM1777	SO	309100	241400	0.69
BRM1720	SN	277600	245800	0.28	BRM1778	SO	307400	241600	0.46
BRM1721	SN	281200	240300	0.57	BRM1779	SN	286710	247730	0.48
BRM1722	SN	282400	241300	0.43	BRM1780	SN	285680	247580	0.35
BRM1723	SN	283200	242600	0.53	BRM1781	SN	284200	246690	0.51
BRM1724	SN	284800	244000	0.34	BRM1782	SN	286190	246710	0.43
BRM1725	SN	287800	246700	0.53	BRM1783	SN	285910	252200	0.46
BRM1726	SO	303700	250800	0.31	BRM1784	SN	287360	252080	0.45
BRM1727	SO	301000	250200	0.32	BRM1785	SN	281780	255200	0.29
BRM1728	SN	299700	249900	0.36	BRM1786	SN	282410	254100	0.29
BRM1729	SN	298300	249400	0.38	BRM1787	SN	283020	252260	0.32
BRM1730	SN	296400	248400	0.37	BRM1788	SN	282720	257520	0.32
BRM1731	SN	296200	247400	0.39	BRM1789	SN	286280	256070	0.26
BRM1732	SN	297600	246100	0.42	BRM1790	SN	285150	255930	0.35
BRM1733	SN	298900	244600	0.44	BRM1791	SN	284780	257600	0.16
BRM1734	SO	300800	240800	0.67	BRM1792	SN	286400	258300	0.20

Sample No.	Square	Easting	Northing	IC	Sample No.	Square	Easting	Northing	IC
BRM1793	SN	285500	257110	0.34	BRM1817	SN	289150	255380	0.51
BRM1794	SN	284500	248280	0.46	BRM1818	SN	288800	257880	0.27
BRM1795	SN	283500	247900	0.44	BRM1819	SN	288300	256500	0.35
BRM1796	SN	281960	248380	0.35	BRM1820	SN	291540	257550	0.56
BRM1797	SN	281700	246190	0.39	BRM1821	SN	292330	258600	0.48
BRM1798	SN	281950	244890	0.61	BRM1822	SN	291500	257680	0.52
BRM1799	SN	281280	243070	0.59	BRM1823	SN	292610	256810	0.46
BRM1800	SN	283960	244800	0.32	BRM1824	SO	309160	248480	0.45
BRM1801	SN	299680	252580	0.45	BRM1825	SO	309690	250850	0.47
BRM1802	SN	298220	253030	0.51	BRM1826	SO	308590	244870	0.46
BRM1803	SN	297620	255210	0.66	BRM1828	SO	307910	252920	0.52
BRM1804	SN	296560	254620	0.70	BRM1829	SN	286290	258000	0.27
BRM1805	SN	295380	256400	0.49	BRM1830	SN	283580	242950	0.46
BRM1806	SN	294630	254800	0.57	BRM1831	SN	283450	242930	0.44
BRM1807	SN	293390	254830	0.50	BRM1832	SN	286250	247320	0.32
BRM1808	SN	293790	252110	0.54	BRM1833	SN	286260	246670	0.48
BRM1809	SN	292040	253890	0.58	BRM1834	SN	285420	254410	0.24
BRM1810	SN	287980	244750	0.54	BRM1835	SN	296250	246710	0.36
BRM1811	SN	288280	241760	0.82	BRM1836	SN	289050	243450	0.60
BRM1812	SN	292720	243690	0.36	BRM1837	SN	284290	240520	0.59
BRM1813	SN	294040	244840	0.46	BRM1846	SO	303210	250810	0.42
BRM1814	SO	308290	257870	1.16	BRM1847	SN	291890	255140	0.30
BRM1815	SO	308480	257850	1.17	BRM1848	SN	291250	255380	0.32
BRM1816	SO	308900	256610	1.05	BRM1849	SN	290380	256380	0.38